

## Modeling of the mechanical properties of polylactic acid/clay nanocomposites using composite theories

Aswini Kumar Mohapatra · Smita Mohanty ·  
S. K. Nayak

Received: 20 February 2012 / Accepted: 27 February 2012 / Published online: 13 April 2012  
© Central Institute of Plastics Engineering & Technology 2012

**Abstract** The mechanical properties of polylactic acid (PLA)/nanoclay were examined using the composite theories. Among Guth equation, Halpin-Tsai Equation and Modified Halpin-Tsai equation, the Halpin-Tsai equation is universally used for composites reinforced by fiber-like or rod-like fillers. A brief comparison made for the Young's modulus of the platelet-like fillers between the theoretical and experimental data. The experimental procedure followed for the determination of the aspect ratio statistically through the analysis of transmission electron microscope (TEM). The modulus reduction factor (MRF) is more significant towards the improvement of predicted theoretical values of the modulus. By introducing the modulus reduction factor (MRF) the polymer-clay nanocomposites was better explained through the composite theory.

**Keywords** Modelling · Composites · Polymer nanocomposites · TEM

### Introduction

In last 10 years, the consumption of biodegradable materials increased 15times as a new group of products. Now-a-days, Bio-degradable materials are used in specialist industry (tissue engineering), in mass production (packaging) and also have been applied as modifiers accelerating decomposition of synthetic polymers in natural environment [1, 2]. Among the biodegradable polymers, aliphatic polyester is one

---

A. K. Mohapatra · S. Mohanty · S. K. Nayak (✉)  
Laboratory for Advanced Research in Polymeric Materials (LARPM), Central Institute of Plastics  
Engineering and Technology, Bhubaneswar 751024 Odisha, India  
e-mail: drsknayak@gmail.com

A. K. Mohapatra  
e-mail: aswini\_cet@yahoo.co.in

S. Mohanty  
e-mail: larpmcipet@gmail.com

of the most promising biodegradable materials because they are readily susceptible to biological attack [3–5].

Poly (lactic acid) (PLA), a biodegradable aliphatic polyester, produced from renewal resources has received much attention in the research of alternative biodegradable polymers [6, 7]. This PLA polymer is the most popular polymer in the world and may be processed using standard machines, equipments and technologies for classic polymers [8–15]. PLA shows good biocompatibility and physical properties, such as high mechanical strength, thermoplasticity and fabricability [16].

Most applications of PLA would be increased by the reinforcement of nanostructured fillers such as carbon nanotubes, nanoclays and nanoparticles etc. Reinforcement is usually associated with improvement in modulus, hardness and tensile strength of material. Polymer-layered silicate nanocomposites have attracted much attention recently, because of their outstanding mechanical properties and low gas permeability [17–20]. Layered silicates composed of sheet-like platelets that are about 1 nm in thickness and 100–1,000 nm in width and length. So they possess very high aspect ratios and large surface areas. Due to the high aspect ratios and good planar orientation, nanoparticles are proven to be good reinforcing agents in polymeric materials [21]. Among all nanoparticle reinforced composites, the most widely investigated systems are based on silicates and clay particles. Ahn et al. reported that the tensile modulus of composites reinforced with unmodified silica nanoparticles improved upon increasing the silica content, however, the elongation to failure decreased [22]. A Toyota research group developed an economic industrial process for the manufacture of polymer/clay nanocomposites. This work led to the development of composites with twice the Young's modulus as that of the pure polymer. The increase in Young's modulus was also observed at elevated temperatures [23, 24].

In the past few years, a considerable amount of research has been conducted to examine the modelling of mechanical properties of polymer composites with nanoscale reinforcement. The majority of mechanical properties of polymer composites elaborated with nanoscale reinforcement. The majority of work has focused on carbon nanotube reinforced polymers [25–30]. Even though it has been shown that these materials have the potential to have excellent mechanical properties, the relatively high costs of development and manufacturing of nanotube/polymer composites has been prohibitive. A lower cost approach is the use of clays and particles in the polymer. Several efforts have focused on modelling of mechanical properties of nanoclay reinforced polymer composites [31] and nanoparticle reinforced polymer composites [32, 33]. Further, the above modeling efforts have demonstrated the need for the development of a model that will predict the mechanical properties of the nanoclay/poly(lactic acid) composites as a function of the nanoclay size and volume fraction.

In the present investigation the PLA/nanoclay composites have been prepared using melt blending technique. The purpose of this paper is to evaluate whether the reinforcing efficiency of PLA nanocomposites can be explained using the composite theories, Guth [34], Halpin-Tsai [35, 36] and the modified Halpin-Tsai equations [37, 38]. Comparison are made between the experimental data and model predictions for PLA/Clay nanocomposites and some interesting results have been acquired.

## Experimental

### Materials

Polylactic acid PLA 4042D nature work with  $1.24 \text{ g/cm}^3$  as density was used. The resin was provided in the form of granules. Two types of organoclay under commercial names of closite 93A (C93A) modified with methyl dehydrogenated tallow ammonium having CEC 90 meq/100 g clay and closite 30B (C30B) modified with methyl bis-2-hydroxyethyl hydrogenated tallow ammonium having CEC of 90 meq/100 g clay were supplied by Southern Clay Products Inc. (Gonzalez, Tx).

### Preparation of nanocomposites

PLA/organoclay nanocomposites were prepared in a counter rotating batch mixer Haake polylab OS Rheodrive 16 (M/s Thermoscientific, Germany) using melt blending technique with a rotational speed of 40 rpm for 5 min., at a temperature of  $180 \text{ }^\circ\text{C}$ .

Prior to processing, PLA was dried at  $50 \text{ }^\circ\text{C}$  for 6–8 h and the nanoclay was dried at  $80 \text{ }^\circ\text{C}$  for 10–12 h. respectively. Subsequently the melt mixes brought to room temperature & compression molded at  $180 \text{ }^\circ\text{C}$  and 120Mpa (M/s Neoplast, Mumbai). Specimens were prepared using counter cut copy milling machine (M/s Ceast, Italy) for testing and characterization.

### Mechanical properties

PLA nanocomposites sample specimens of dimension  $167 \times 12.7 \times 3 \text{ mm}$  were subjected to tensile test, using universal testing machine (UTM, Instron 3386, UK) as per ASTM D638, at crosshead speed of 5 mm/min and gauge length of 50 mm.

### Transmission electron microscopy

The nanoscale morphology of PLA nanocomposites have been studied using transmission electron microscope (JEOL-1200EX, Japan). Samples for TEM imaging were sectioned using Leica ultracut UCT microtome at room temperature, using a diamond knife (M/s Leica, UK). Sections of 50–70 nm thickness were collected from water on 300-mesh carbon-coated copper grids and kept overnight on filter paper for drying. Subsequently, TEM of the sections was carried out using the electron microscope at an accelerating voltage of 100KV.

### X-ray diffraction (XRD)

X-ray diffraction (XRD) analysis was carried out using XRD-7000, M/s Shimadzu, Japan which have a monochromator and a Cu radiation source of wave length  $1.54 \text{ \AA}$  operating at 40 kV and 30 mA. The basal spacing or d-spacing ( $d_{001}$ ) reflection of the

clay gallery and the PLA based nanocomposites was calculated using Bragg's law equation (i.e.  $n\lambda=2d\sin\theta$ ) by monitoring the diffraction angle  $2\theta$  from  $2^\circ$  to  $10^\circ$  with a scanning rate of  $2^\circ/\text{min}$ .

## Modeling method overview and back ground

The importance of modeling in understanding of the behavior of matter is illustrated in Fig. 1. The earliest attempt to understanding material behavior is through observation via experiments. Careful measurements of observed data are subsequently used for the development of models that predict the observed behavior under the corresponding conditions. The models are necessary to develop the theory. The theory is then used to compare predicted behaviour to experiments via simulation. This comparison serves to either validate the theory, or to provide a feedback loop to improve the theory using modeling data. Therefore, the development of a realistic theory of describing the structure and behaviour of materials is highly dependent on accurate modeling and simulation techniques.

In order to correlate the experimental observations, several micromechanical models have been developed to predict the macroscopic rigidity improvement of the nanocomposites. The reviews of these models have been prepared by Ahmed et al. In 1990 [40] and more recently by Tjong [41]. These models are based on either a two-phase or a three-phase approach.

The particle/matrix two phase systems is the earliest and most popular theory of Einstein [42], which was developed for composites with spherical rigid inclusions in a non-rigid matrix. Several developments have been made covering a wide variety of composites, and involving both series and parallel models [34, 43–50]. Both, Kaplan [49] and Hansen [50] proposed models that predicted the modulus enhancement of polymer composites formed by rigid inclusions in a rigid matrix. In 1945 Guth [34] proposed a phenomenological model for predicting the stiffness of polymer

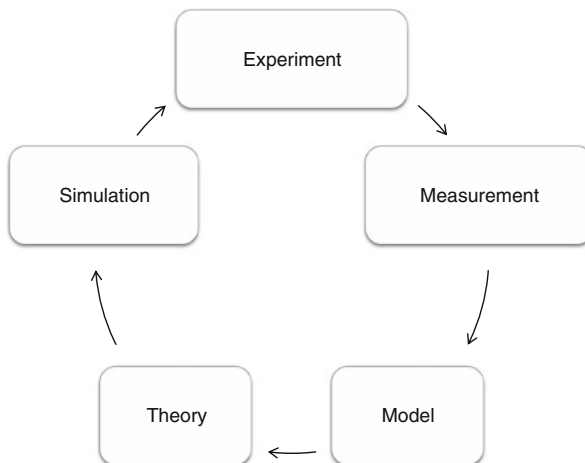


**Fig. 1** Schematic diagram of the process of developing theory and the validation of experimental data [adopted from [39]]

composites, and which was more generalised in nature. This express the ratio of the young's modulus  $E_c$  of the composite to that of matrix, under a second order polynomial function of volume fraction filler  $\emptyset$ .

$$E_c/E_m = 1 + 2.5\emptyset + 14.1\emptyset^2 \quad (1)$$

The volume fraction of each nanoreinforcement was calculated using Eq. [2] [30].

$$\emptyset = (w_r/\rho_r)/[(w_r/\rho_r) + (1 - w_r)/\rho_m] \quad (2)$$

Where,  $w_r$ = weight fraction of nanoreinforcement,  $\rho_{PLA}=1.24 \text{ g/cm}^3$ ,  $\rho_{C93A \text{ Clay}}=1.88 \text{ g/cm}^3$  and  $\rho_{C30B \text{ Clay}}=1.98 \text{ g/cm}^3$  datas were used in the Eq. (2) for calculation.

The Eq. (1) is only applicable to elastomers filled with a certain amount of spherical fillers. In view of high filler concentration i.e. more than 10 volume%, the modulus increases much more rapidly than Eq. (1) would predict. The reason can be attributed to the formation of a network by the spherical filler chains. Considering the chains composed of spherical fillers are similar to rod like filler particles embedded in a continuous matrix. The following equation was being developed later by Guth [34] by introducing a shape factor  $\alpha$  (length/breadth) in order to account for this "accelerated stiffening".

$$E_c/E_m = 1 + 0.67\alpha\emptyset + 1.62(\alpha\emptyset)^2 \quad (3)$$

As shown in Fig. 2, Eq. (3) clearly exhibits a rapid increase of  $E_c$  with increasing filler volume fraction for large  $\alpha$ . The Guth equation is the basic approach towards the composite theory and is mainly applicable to rubber composites. But we have studied this equation for the modelling of young's modulus of PLA/Clay nanocomposites as a trial & verification of the equation adaptability due to the similar accountability of shape factor of stiff particles.

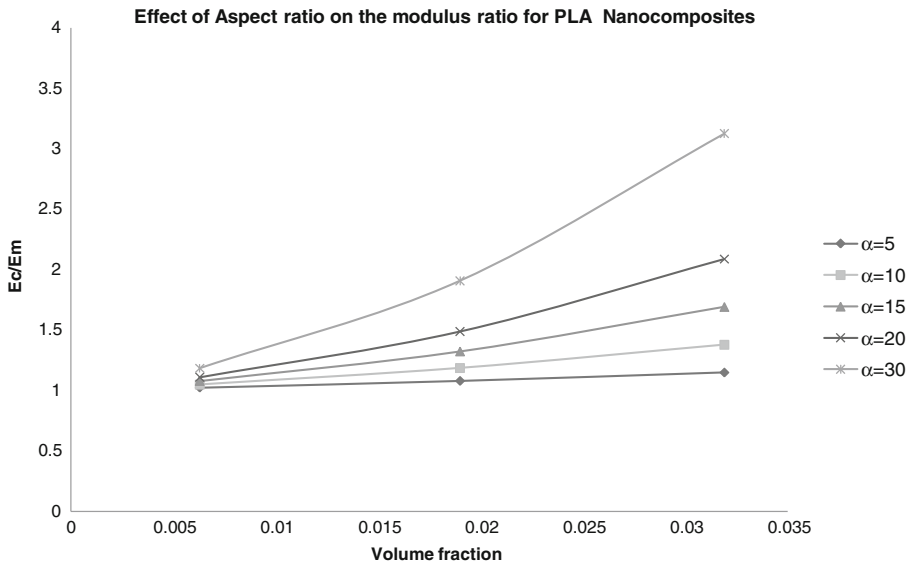


**Fig. 2** Showing effect of aspect ratio on the modulus ratio (Guth equation)

Further, Halpin-Tsai expressed the equation to estimate reinforcement effects of filler in composites and which was also widely used for the study of various reinforced composites. So Halpin-Tsai and modified Halpin-Tsai equations are taken into consideration for the study in this work. The elastic modulus of composite materials reinforced by discontinuous cylindrical fibers or lamellar shapes is expressed in the same form [35, 36], as mentioned in the below equation:

$$E_c/E_m = (1 + \xi\eta\varnothing)/(1 - \eta\varnothing) \quad (4)$$

In Eq. (4),  $\xi$  is a shape parameter dependent upon filler geometry, orientation and loading direction. The constants  $\xi$  and  $\eta$  are given by:

$$\xi = 2(l/d) \\ \eta = [(E_f/E_m) - 1]/[(E_f/E_m) + \xi]$$

Where,  $E_f$  and  $(l/d)$  represents young's modulus and the aspect ratio of the fillers respectively.

Equation (4) of Halpin and T-sai was subsequently extended by Nielsen to nanocomposites (modified Halpin-Tsai equation) with dispersed clay particles without intercalation, and was rewritten as follows [51]:

$$E_c/E_m = (1 + \xi\eta\varnothing)/(1 - \Psi\eta\varnothing) \\ \Psi = 1 + \varnothing[(1 - \varnothing_m)/\varnothing_m^2] \\ \eta = [(E_f/E_m) - 1]/[(E_f/E_m) + \xi] \quad (5)$$

$E_f$  is the young's modulus of the clay and generally assumed to be equal to  $\approx 170$ Gpa [52].

$\varnothing$  and  $\varnothing_m$  are the volume fractions of clay reinforcement and the maximum packing volume fraction (true volume of the filler/apparent volume occupied by the filler) of clay respectively.

Figures 3 and 4 show the effect of aspect ratio on the modulus in Eqs. (4) and (5), respectively. In comparison to Fig. 3, Fig. 4 shows a rapid increase of modulus with increasing concentration for large  $\alpha$  at high filler concentration by introducing  $\Psi$ . Hence Eq. (5) can be applied to predict the modulus of nanocomposites over a wide range of filler concentration.

Figure 5 shows the effect of the maximum volumetric packing fraction  $\varnothing_m$  of the filler on the modulus ratio in the modified Halpin-Tsai equation. It is observed that the smaller  $\varnothing_m$ , the faster increase of modulus ratio, demonstrating the contribution of the apparent volume occupied by the filler. It is assumed that the filler apparent volume is related to the dispersion of filler, and the larger apparent volume may originate in better filler dispersion, which results in the higher modulus of the composite.

## Results and discussion

### Determination of the aspect ratio of clay inclusion

The aspect ratio of clay platelets must be determined to model the modulus of PLA/Clay nanocomposites. The TEM method is used to analyze the aspect ratio of the

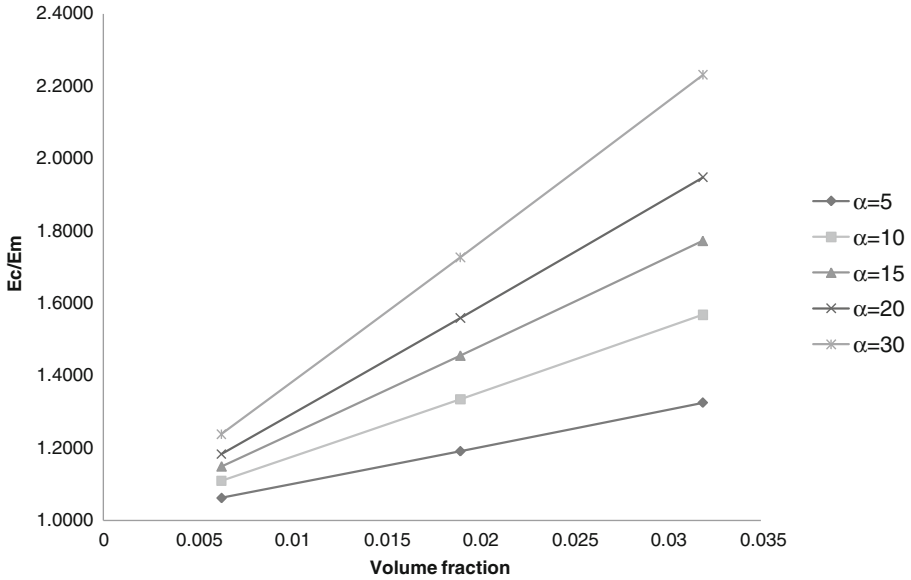


Fig. 3 Showing effect of aspect ratio on the modulus ratio (Halpin-Tsai equation)

nanoclays statistically through its micrographs [53, 54]. Figure 6 shows the typical TEM bright field image of PLA nanocomposites where the dispersion and orientation of clays in polylactic acid were examined. In these TEM photographs, the light regions and dark bands represent the matrix polymer and Organoclay particles, respectively. The dark entities are the cross-section of intercalated silicate layers [25–28]. The PLA molecules separate the clay particles into either individual layers

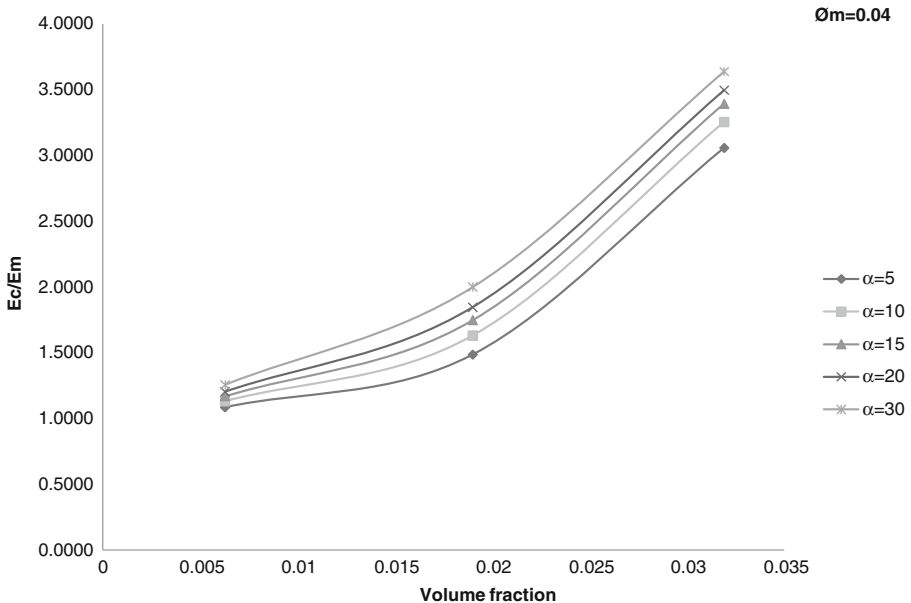
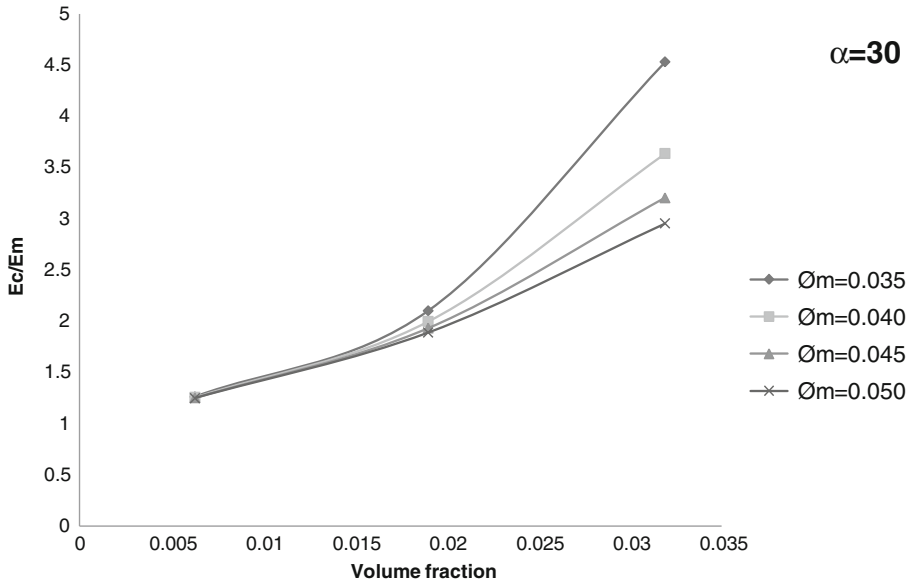
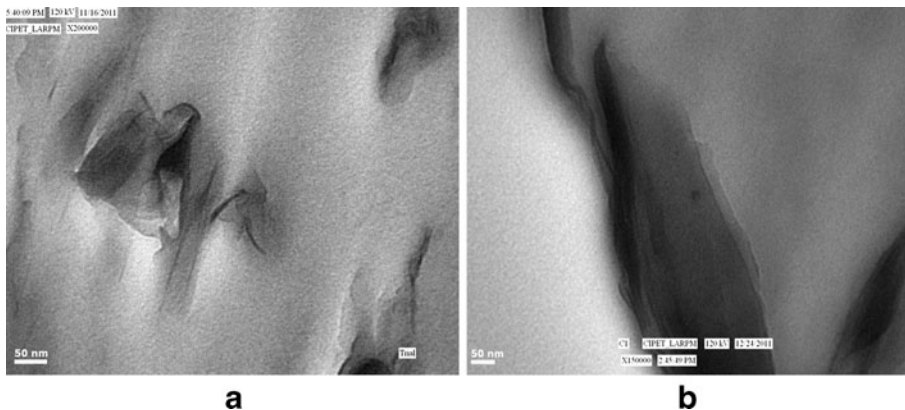


Fig. 4 Showing effect of aspect ratio on the modulus ratio (Modified Halpin-Tsai equation)



**Fig. 5** Showing effect of the maximum volumetric packing fraction  $\varnothing_m$  of the filler on the modulus ratio (Modified Halpin-Tsai equation)

or just silicate layer aggregates of nanometre thickness. Further, the silicate layers have good plane orientation. Therefore, the aspect ratio of clay inclusions should be directly calculated by measuring the length and thickness of the dark lines in TEM micrographs at different magnifications [53]. In fact, The accurate and reliable automated analysis of TEM photomicrographs demands an original image having exceptional resolution and contrast. But, generally a large majority of TEM images consist of different shades of gray, which makes it very difficult to conduct automated image analysis. The calculation of aspect ratio of dark lines corresponding to silicate layers is based on their measurement of the length and thickness manually. But it is a time-wasting process to measure them one by one through a naked eye. The statistical data of the aspect ratio for PLA nanocomposites are shown in Fig. 7. These data were



**Fig. 6** TEM micrographs of (a) PLA/C30B an (b) PLA/C93A



obtained by measuring many TEM photographs of the nanocomposites having different clay contents due to the small variation of the aspect ratio with the filler concentration [55, 56].

Determination of the modulus reduction factor (MRF) for the platelet-like fillers

As the Halpin-Tsai equations remain in the same form for discontinuous fibers and lamellar shape reinforcements and, moreover, the silicate layers exhibit good planar orientation. Halpin-Tsai equations could be directly applied to predict the modulus of the layered silicate composites. A comparison made between the experimental data of PLA/C30B clay nanocomposites and modulus prediction by the Halpin-Tsai equation. Here, PLA/C30B clay nanocomposites experimental data has been taken for the determination of MRF in comparison to the theoretical prediction by the Halpin-Tsai equation due to the better exfoliation/intercalated characteristics of C30B clay with the PLA matrix as compared to the C93A clay with the PLA matrix which was clearly evident from the XRD analysis. The XRD patterns of the organoclays (C30B and C93A) and PLA nanocomposites are shown in Fig. 8(a) and (b) respectively.

In case of PLA/C30B nanocomposites, a small peak was observed at low-angle range which confirms the intercalation of silicate layers of C30B in PLA matrix after

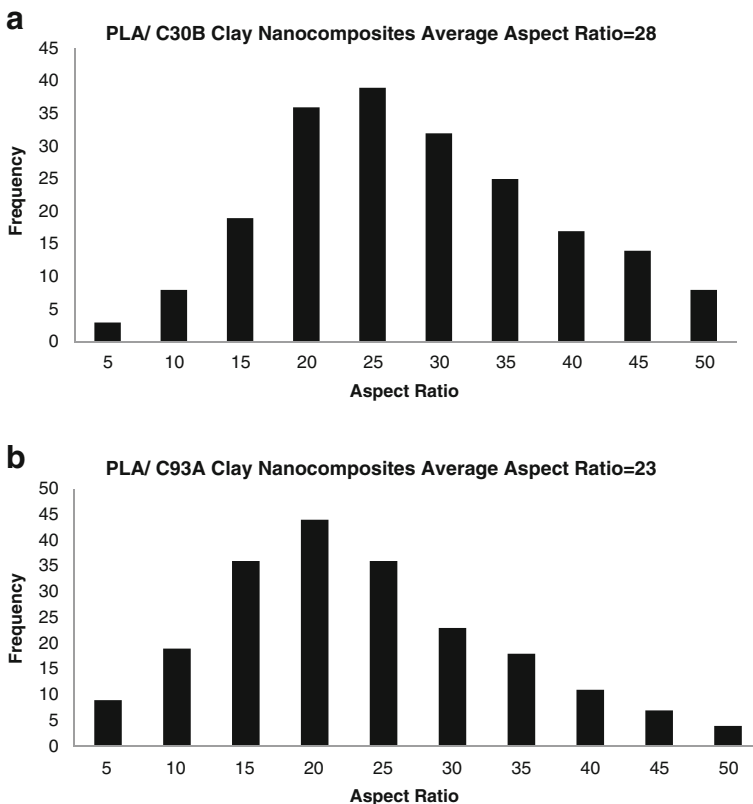


**Fig. 7** Showing aspect ratio of clay Platelets in (a) PLA/C30B clay Nanocomposites and (b) PLA/C93A clay Nanocomposites

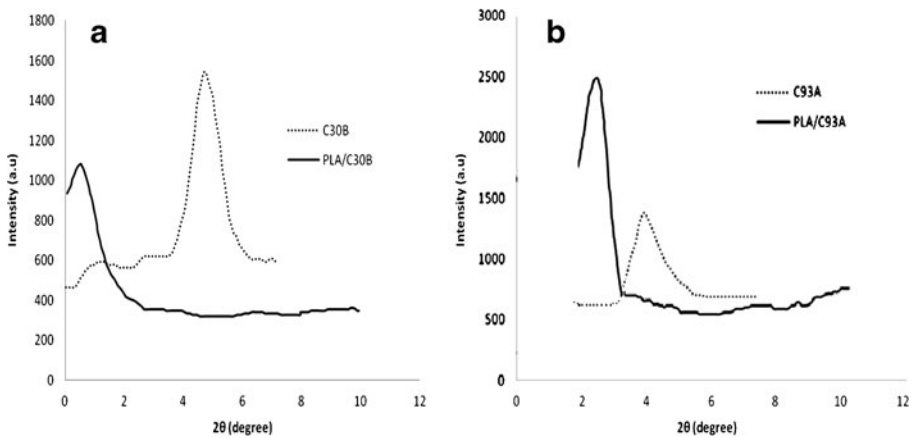


**Fig. 8** (a) and (b). WAXD diffractograms of C30B and PLA/C30B, and C93A and PLA/C93A respectively

the melt mixing. The lack of intergallery clay diffraction is due to the disorderly and random distribution of the clay platelets within the PLA matrix. In contrast to PLA/C30B, PLA/C93A nanocomposites shows a high diffraction peak after melt mixing with PLA at high intensity level. There is a shifting of the diffraction peak to lower angle at  $2\theta=3.8^\circ$  (d-spacing $\approx 2.32$  nm) to  $2\theta=2.9^\circ$  (d-spacing $\approx 3.04$  nm) in case of C93A and PLA/C93A respectively. This indicates that the layer spacing of C93A was slightly increased but its ordered structure was not disrupted after melt mixing. Another small peak is also observed in case of PLA/C93A due to the second registry of MMT clay [57, 58].

From the above XRD analysis, we can conclude that PLA/C30B shows the better characteristics in respect of the compatibility and intercalation of the clays with the PLA matrix after melt mixing. Whereas, PLA/C93A was not exfoliated or significantly intercalated after mixing with PLA. The same observations were also attributed in case of PCL/C30B and PCL/C93A hybrids [59]. This behaviour is primarily due to the hydrophilic nature of C30B clay, and the formation of hydrogen-bond between the carbonyl group in the main chain of PLA molecules and the hydroxyl group in the organic modifier of C30B. On the contrary, the C93A nanoclay has no polar interaction because of its nonpolar organic modifier.

It is depicted from the Fig. 9 that the predicted moduli by Halpin-Tsai equation are higher than the experimental data. This could be attributed to the contribution of plate-like clay (two dimension) to modulus being less than a fibre like dispersed phase (one dimension) [60]. In the theories of the modulus prediction, the assumption of the morphology difference between the plate-like-filler and the fiber-like filler phase is neglected and which should be taken into account. Therefore, we introduced the “modulus reduction factor (MRF)” for the platelet like fillers. As the MRF is related to the morphology of the filler, MRF should appear together with the aspect ratio. An improvement is to be expected in Halpin-Tsai equation after introducing the MRF for the predicting ability of the moduli.

As shown in Fig. 9, when the MRF value is of 0.66, the predicted values at filler concentration of less than 3 wt% is well fitted to the experimental data.

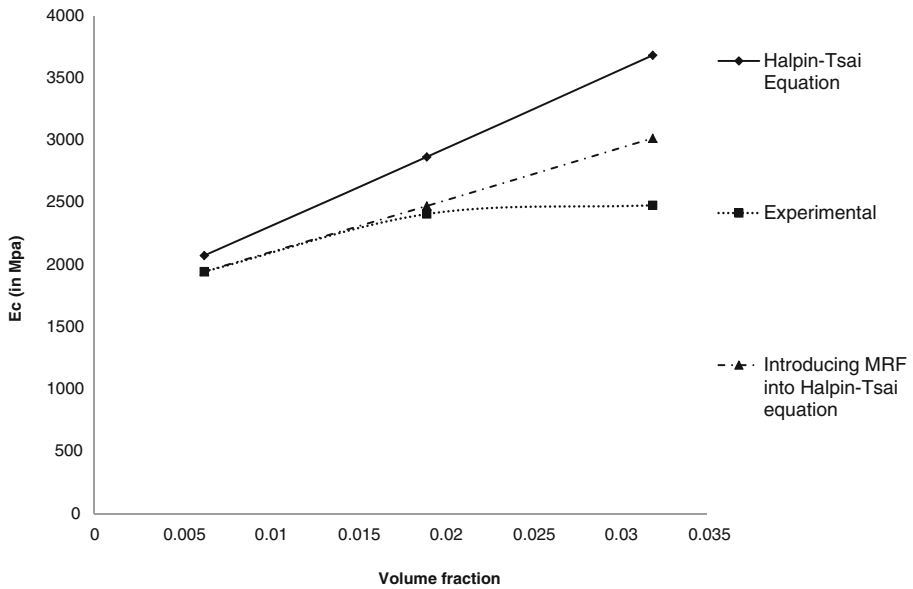


**Fig. 9** Showing the comparison of experimental data of PLA/C30B clay nanocomposites and theoretical prediction for the determination of MRF

Comparison between experimental data and predictions by introducing MRF

The Guth, Halpin-Tsai and modified Halpin-Tsai equations are transformed into the following equations respectively after introducing MRF:

[where  $\eta = [(E_f/E_m) - 1]/[(E_f/E_m) + \xi]$  and  $\xi = 2\alpha$  for Eqs. (7) and (8)].

$$E_c = E_m \left[ 1 + 0.67(\text{MRF})\alpha\theta + 1.62(\text{MRF})^2\alpha^2\theta^2 \right] \tag{6}$$

$$E_c/E_m = (1 + 2(\text{MRF})\alpha\eta\theta)/(1 - \eta\theta) \tag{7}$$

$$E_c/E_m = (1 + 2(\text{MRF})\alpha\eta\theta)/(1 - \Psi\eta\theta) \tag{8}$$

**Table 1** Young’s modulus of PLA nanocomposite compositions

Sample details	Young’s modulus (Mpa)
PLA	1690
PLA/1%C93A	1901
PLA/3%C93A	2295
PLA/5%C93A	2362
PLA/1%C30B	1947
PLA/3%C30B	2410
PLA/5%C30B	2480

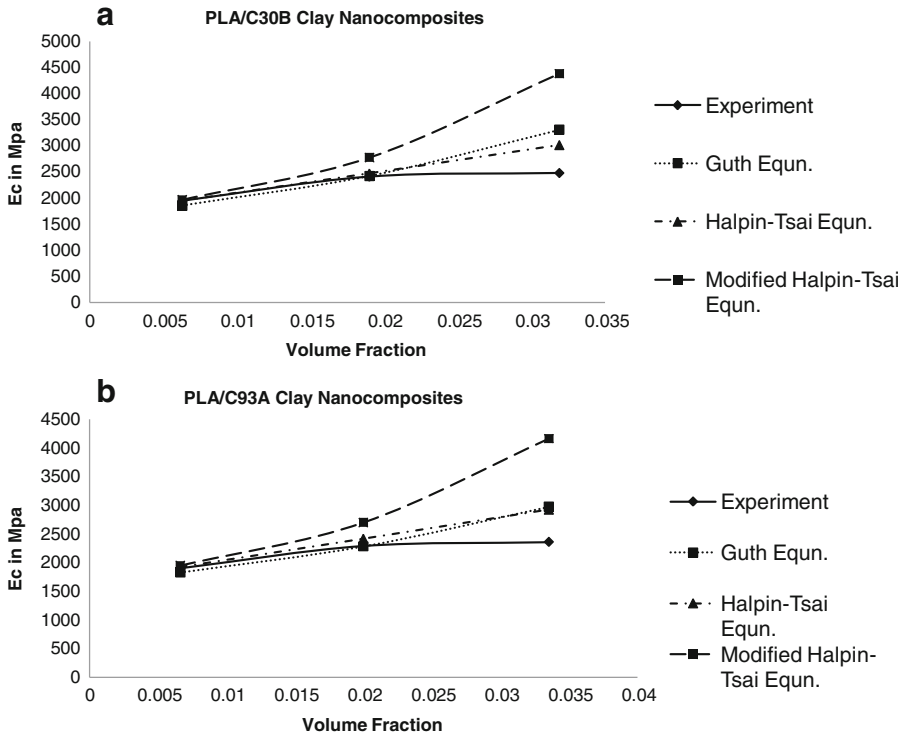


**Fig. 10** Showing comparison between experimentally measured Young’s modulus data with theoretical predictions by the three equations after introducing MRF 0.66 for (a) PLA/C30B Clay Nanocomposites and (b) PLA/C93A Clay Nanocomposites

In Eq. (8),  $\Psi = 1 + \phi [(1 - \phi_m) / \phi_m^2]$  where  $\phi_m$  is determined by fitting the experimental data to theoretical predictions in our study.

The experimental results of tensile modulus for PLA/Clay nanocomposites are as shown in Table 1. Figure 10 compares experimental modulus data of PLA nanocomposites with the model predictions using the parameter values in Table 2. Even though, the Guth equation is only applicable to elastomeric composites, but in this case the theory is providing a little idea of comparable results with the experimental data after introducing the MRF 0.66 into the equation. Hence the illustration made for the Halpin-Tsai and modified Halpin-Tsai predictions. The Halpin-Tsai equation resembles very well with the experimental data in the range of low clay volume fraction to predict the modulus of PLA/Clay nanocomposites; whereas the modified Halpin-Tsai has large potential which this experiment was unable to reach. By

**Table 2** Parameter values for theoretical predictions

Sample details	$\phi_m$	Aspect ratio ( $\alpha$ )	MRF
PLA/C93A	0.050	23	0.66
PLA/C30B	0.045	28	0.66

introducing MRF the predicting ability of the equations improved. Moreover, MRF for the platelet-like filler is applicable to all the equations. Further, it is depicted from Table 2 that the  $\varnothing_m$  decreased with increase of aspect ratio  $\alpha$ , representing that the clay inclusions with larger aspect ratio possessed higher apparent volume, as would be expected.

Further, a modulus reduction factor (MRF) of 0.66 introduced in this study due to the difference between the regular filler and layered silicate clays which were also evident in the study of Nylon6/clay nanocomposites by Paul et al. [53] and in the study of rubber-clay nanocomposites by Wu et al. [61]. Hence, by introducing 0.66 as MRF into the Halpin-Tsai equation, the predicted values are a better fit with the experimental data than those of the original Halpin-Tsai equation.

## Conclusion

The modelling of polymer based nanocomposites has become an important topic in recent times because of the need for the development of these materials for various applications. The mechanical modelling of polymer nanocomposites plays a vital role in respect of the study of Young's modulus through the various composite theories. The modulus reduction factor (MRF) for platelet-like fillers was introduced into the composite theories of polymer clay nanocomposites.

The introduction of MRF in the equations enhances the theoretical prediction ability of Young's modulus in comparison to the experimental values. The 0.66 MRF shows the better results in the improvement of the equations for polymer clay nanocomposites. The Halpin-Tsai equation can be applied to predict the modulus of PLA/Clay Nanocomposites with low clay volume fractions and the PLA/C30B clay nanocomposites resembles more than the PLA/C93A clay nanocomposites.

## References

1. Kaczmarek H, Barej K (2008) *Polim* 9:631
2. Bajer K, Kaczmarek H, Dzwonkowski J, Stasiek A, Oldak D (2007) *J Appl Polym Sci* 103:2197
3. Hwang KJ, Park JW, Kim IL, Ha CS, Kim GH (2006) *Macromol Res* 14:179
4. Lee Y, Chang JB, Kim HK, Park TG (2006) *Macromol Res* 14:359
5. Sato H, Murakami R, Zhang J, Ozaki Y, Mori K (2006) *Macromol Res* 14:408
6. Tsuji H, Ikada Y (1998) *J Appl Polym Sci* 67:405
7. Perego G, Cella GD, Bastioli C (1996) *J Appl Polym Sci* 59:37
8. Bledzki A, Fabrycy E (1992) *Polim* 37:343
9. Garlotta D (2001) *J Polym Environ* 9:63
10. Foltynowicz Z, Jakubiak P (2002) *Polim* 47:769
11. Duda A, Penczek S (2003) *Polim* 48:16
12. Pinkowska E (2006) *Polim* 51:836
13. Golebiewski J, Gibas E, Malinowski R (2008) *Polim* 53:799
14. Lim LT, Auras R, Rubino M (2008) *Prog Polym Sci* 33:820
15. Jiang L, Wolcott MP, Zhang J (2006) *Biomacromol* 7:199
16. Cai H, Dave V, Gross RA, McCarthy SP (1996) *J Polym Sci B Polym Phys* 34:2701
17. Kojima Y, Usuki A, Kawasumi M, Okada A, Kurauchi T, Kamigaito O (1993) *J Appl Polym Sci* 49:1259
18. Messersmith PB, Giannelis EP (1995) *J Polym Sci A Polym Chem* 33:1047

19. Giannelis EP (1996) *Adv Mater* 8:29
20. Vala RA, Price G, Ruth PN, Nguyen HT, Lichtenhan J (1999) *J Appl Clay Sci* 15:67
21. Shepard PD, Golemba FJ, Maine FW (1974) *Adv Chem Ser* 134:41
22. Ahn SH, Kim SH (2004) *Macromol Res* 12:293
23. Usuki A, Kojima Y, Kawasumi M, Okada A, Fukushima Y, Kurauchi T, Kamigaito O (1993) *J Mater Res* 8:1179
24. Kojima Y, Usuki A, Kawasumi M, Okada A, Fukushima Y, Kurauchi T, Kamigaito O (1993) *J Mater Res* 8:1185
25. Frankland SJV, Caglar A, Brenner DW, Griebel M (2002) *J Phys Chem B* 106:3046
26. Bradshaw RD, Fisher FT, Brinson LC (2003) *Compos Sci Tech* 63:1705
27. Fisher FT, Bradshaw RD, Brinson LC (2003) *Compos Sci Tech* 63:1689
28. Frankland SJV, Harik VM, Odegard GM, Brenner DW, Gates TS (2003) *Compos Sci Tech* 63:1655
29. Odegard GM, Frankland SJV, Gates TS (2003) 44th AIAA/ASME/ASCE/AHS structures, structural dynamics, and material conference. Norfolk
30. Odegard GM, Gates TS, Wise KE, Park C, Siochi E (2003) *Compos Sci Tech* 63:1671
31. Sheng N, Boyce MC, Parks DM, Rutledge GC, Abes JI, Cohen RE (2004) *Polym* 45:487
32. Smith GD, Bedrov D, Li L, Bytner O (2002) *J Chem Phys* 117:9478
33. Brown D, Mele P, Marceau S, Alberola ND (2003) *Macromol* 36:1395
34. Guth E (1945) *J Appl Phys* 16:20
35. Halpin JC, Kardos JL (1976) *Polym Eng Sci* 16:344
36. Halpin JC, Compos J (1969) *Compos Mater* 3:732
37. Nielsen LE (1970) *J Appl Phys* 41:4626
38. Lewis TB, Nielsen LE (1970) *J Appl Polym Sci* 14:1449
39. Gates TS, Hinkley JA (2003) NASA/TM-212163
40. Ahmed S, Jones FR (1990) *J Mater Sci* 25:4933
41. Tjong SC (2006) *Mater Sci Eng* 53:73
42. Einstein A (1956) *Investigations on the theory of the Brownian movement*. Dover, New York
43. Money M (1951) *J Coll Sci* 6:162
44. Brodnyan JG (1959) *Trans Soc Rheol* 3:61
45. Broutman LJ, Krock RH (1967) *Modern composite materials*. Addison Wesley, Reading
46. Hirsch TJ (1962) *J Am Concr Inst* 59:427
47. Paul B (1960) *Trans Am Inst Min Metall Eng* 218:36
48. Counto UJ (1964) *Mag Concr Res* 16:129
49. Kaplan MF (1959) *Bull RILEM. Paris* 1:58
50. Hansen TC (1965) *J Am Concr Inst* 62:193
51. Nielsen LE (1981) *Mechanical properties of polymer and composites vol 2*. Marcel Dekker, New York
52. Somoza AM, Tarazona P (1989) *J Chem Phys* 91:517
53. Fornes TD, Paul DR (2003) *Polym* 44:4993
54. Jeon HS, Rameshwaram JK, Kim G (2004) *J Polym Sci B Polym Phys* 42:1000
55. Fornes TD, Yoon PJ, Keskkula H, Paul DR (2001) *Polym* 42:9929
56. Fornes TD, Yoon PJ, Keskkula H, Paul DR (2002) *Polym* 43:2121
57. Ray SS, Okamoto M (2003) *Prog Polym Sci* 28:1539
58. Ray SS, Maiti P, Okamoto M, Yamada K, Ueda K (2002) *Macromol* 35:3104
59. Pluta M, Galeski A, Alexandre M, Paul MA, Dubois P (2002) *J Appl Polym Sci* 86:1497
60. Oberth AE (1967) *Rubber Chem Tech* 40:1337
61. Wu YP, Jia QX, Yu DS, Zhang LQ (2004) *Polym Test* 23:903